


# Pt/C, Au/C and Pd/C Catalysts for Alkaline-based Direct Glycerol Fuel Cells

Elcio Frota Jr, Ângelo Purgatto, José J. Linares\*

  
 Instituto de Química, Universidade de Brasília, Campus Darcy Ribeiro CP 4478 70910-900, Brasília, Distrito Federal,  
 Brazil  
 \*joselinares@unb.br

This study presents the results of the preparation of monometallic catalysts for glycerol electrooxidation by simple chemical reduction methods: formic acid for Pt, citrate-assisted NaBH<sub>4</sub> for Au and ammonia-assisted NaBH<sub>4</sub> for Pd. The metal nanoparticles, within a range of 3-7 nm, anchor successfully, as demonstrated by thermogravimetry and EDS analyses, and spread, as displays by the TEM images, on the carbon support. The XRD patterns display the fcc crystalline facets, except for the case of Pd/C, where peaks associated to the formation of metastable palladium carbide are present. The electrochemical activity for glycerol oxidation was evaluated in a three electrode glass cell by cyclic voltammetry, revealing that Pt/C possesses the lowest onset potential and Au/C the maximum current density. The Pd/C catalysts also present a electrochemical activity (despite the presence of PdC), with an intermediate onset potential between Au and Pt. Regarding the influence of the metal loading, Pt/C displays the best performance for the high metal loaded 60% Pt/C, whereas for Au/C and Pd/C, lowest loaded 20% Au/C and Pd/C. The direct comparison of these three materials in a chronoamperometric measurement (at -0.2 V vs Hg/HgO) reveals that Pt/C is the most effective material at such more useful potentials. Finally, the product distribution reveals that the metal may be a useful tool for a pre-selection of a particular product.

## 1. Introduction

Despite the notable benefit of the development of the biodiesel industry in the last decade, due to the reduction of the fossil fuel dependence of the automobile sector (Issarihyakul and Dalai, 2014), its synthesis, through a transesterification process produces significant amounts of the by-product glycerol (for each 10 kg of biodiesel, 1 kg of glycerol) (Kiss and Ignat, 2012). The large amounts of glycerol "residue" demands an effective management. Classical industries that used glycerol as an input (agro and food, cosmetic and pharmaceutical) saw surpassed their capacity (Motta et al., 2009). Therefore, new alternatives for glycerol utilization are targeted of study and analyses.

One of these alternatives are the glycerol oxidation, where added value products, such as tartronic, mesoxalic, glyceric and glycolic acid can be obtained (Zhang et al., 2012). Classical routes involve homogenous oxidizing agents, such as HNO<sub>3</sub>, H<sub>2</sub>CrO<sub>4</sub> and KMnO<sub>4</sub> (Zheng et al., 2008). Glycerol, due to its biodegradability, can be also processed by biochemical processes, such as fermentation, in order to obtain one very interesting chemical, 1,3-propanediol, raw matter for the polymer industry (Yazdani and Gonzalez, 2007). Nevertheless, biochemical processes present a rather sluggish and complex kinetics. Heterogeneous catalysis can be a very promising alternative for glycerol oxidation. In this sense, some interesting results have been reported in the literature for the oxidation under oxygen atmosphere in alkaline medium with Pt, Au and Pd catalysts (Beltrán-Prieto et al., 2013).

The satisfactory activity displayed by these catalysts clearly opens the possibility of using glycerol as fuel in a Direct Glycerol Fuel Cell (DGFC), with special emphasis in the alkaline environment. Working in alkaline conditions favours the first dehydrogenation step forming an alkoxide, significantly active in

electrochemical terms (Zhang et al., 2013), and indeed, some interesting results have been already shown in the literature for the three abovementioned materials (Lamy and Coutanceau, 2013).

Herein, this study intends to focus on the aforementioned monometallic materials, Pt/C, Au/C and Pd/C. Catalysts with different metal loadings were prepared by simple chemical reduction routes, and structurally characterised by X-ray Diffraction (XRD), Thermogravimetric analyses (TGA) and Transmission Electron Microscopy (TEM). Afterwards, electrochemical measurements were carried out in a three electrode glass cell in order to assess the activity of the different materials for glycerol electrooxidation by cyclic voltammetry and chronoamperometry. Finally, an idea of the product distribution for each metal catalyst after the chronoamperometric test was achieved by HPLC.

## 2. Experimental

### 2.1 Preparation of the catalyst

a) Preparation of Pt/C catalysts. The Pt/C catalysts were prepared by the chemical reduction with formic acid (Pinheiro et al., 2003). In a typical procedure, for the preparation of 100 mg of catalyst of a certain Pt loading, it was first weighted the carbon support (Vulcan XC-72R) and added to 100 mL of a 0.1 mol L<sup>-1</sup> formic acid solution. Next, the system was heated up to 80°C. Once reached this temperature, the necessary amount of the H<sub>2</sub>PtCl<sub>6</sub> precursor (from a 50 g/L) solution was added in three consecutive additions (each 30 minutes). The system was left for 1 hour at that temperature and afterwards to cool down to room temperature. Catalysts with 20, 30, 40 and 60% Pt/C were prepared.

b) Preparation of Au/C catalysts. The Au/C catalysts were prepared by reduction with NaBH<sub>4</sub> and sodium citrate as stabilizer (Rodrigues de Oliveira, 2013). The reduction medium consisted of 1.6 l of ultrapure water with 0.2 g of sodium citrate. Next, the necessary amount of metal precursor (HAuCl<sub>4</sub>) was added to the reduction medium. The reduction took place after the dropwise addition of a 50 mL solution containing 0.2 g of sodium citrate and 0.06 g of NaBH<sub>4</sub>. An immediate orange colour appeared in the medium (Au nanoparticles). Finally, the required amount of carbon support was added and the system was left for 48 hours in order to guarantee the anchorage of the metal nanoparticles to the carbon support. Catalyst with 10, 20, 30 and 40% Au/C were prepared.

c) Preparation of the Pd/C catalysts. These materials were prepared according to the procedure described by Cheng et al. (2010). In a typical procedure, the necessary amount of PdCl<sub>2</sub> was dissolved in 50 mL of water. In order to increase the solubility of the palladium chloride, it was necessary to add 0.5 mL of HCl (1 mol L<sup>-1</sup>). Next, 1 mL of NH<sub>3</sub> (30% v./v.) was added. In case of appearance of turbidity, the reaction medium was softly heated until disappearance. The necessary amount of carbon support (Vulcan XC-72R) was added to the reaction medium and the system was left for 2 hours under vigorous stirring. The final step is the dropwise addition of 0.5 mL of NaBH<sub>4</sub> (1 mol L<sup>-1</sup>). The system was left overnight to ensure the complete deposition of the metal nanoparticles on the carbon support. Catalysts with 20, 30, 40 and 60% Pd/C were prepared.

After the reduction processes, all the catalysts were filtered and washed thoroughly with ultrapure water. The obtained powders were dried in an oven at 90°C for 2 hours, ground carefully in a mortar and stored for subsequent uses.

### 2.2 Structural and morphological characterisation

The metal loading of the Pt/C and Au/C catalysts were determined by a Thermogravimetric Analysis, heating a sample of the catalyst from room temperature to 900°C in air at a heating rate of 10 °C min<sup>-1</sup>, in a Shimadzu DTG-60 (Japan). In the case of the Pd/C, this study could not be carried out due to the formation and sudden decomposition of PdO at approximately 600 °C (Peuckert, 1985). The final metal percentage was roughly estimated by the final sample weight. The XRD patterns of the catalysts were recorded in a D8 Focus (Rigaku Corp., Japan) from 20 to 80 ° (0.05 ° step, 0.5 ° min<sup>-1</sup>). The samples were irradiated with Cu K<sub>α</sub> radiation (λ = 0.15406 nm). Finally, TEM images of the different catalysts were obtained in a JEOL 1011 microscope, operating at 100 kV.

### 2.3 Electrochemical tests

In order to assess the electrochemical performance of the different catalysts, studies in a three electrode glass cell were carried out. An ultra-thin catalyst layer was deposited on a vitreous carbon electrode (0.385 cm<sup>2</sup>) inserted in a Teflon rod. The preparation consisted of dispersing 1 mg of catalysts in 1 mL of isopropanol. With a chromatographic syringe, 40 µL of the dispersion were deposited on the surface of the

carbon electrode and left to evaporate at room temperature. The counter electrode consisted of a platinized Pt mesh. The reference electrode was a Hg/HgO/KOH(1 mol L<sup>-1</sup>) electrode. Cyclic voltammetry (CV) and chronoamperometric (CA) measurements were carried in a 1 mol L<sup>-1</sup> glycerol and 1 mol L<sup>-1</sup> KOH solution. Voltamperograms were recorded between -0.8 and 0.3 V vs. Hg/HgO electrode after nitrogen purge of the solution. The chronoamperograms were obtained by fixing a potential of -0.2 V vs Hg/HgO for 12 hours. All the electrochemical results were normalized with respect to the mass of deposited noble metal.

### 2.4 Product distribution

In order to determine the glycerol electrooxidation products distribution, HPLC injections were carried out, taking a 2 mL sample after the chronoamperometry. In order to separate the different products, an ion exchange chromatographic column (Polypore-H, Perkin Elmer, 22 cm × 4.6 mm, 10 μm) was used. The mobile phase was 0.025 mol L<sup>-1</sup> H<sub>2</sub>SO<sub>4</sub> at room temperature with a flow rate of 0.075 mL min<sup>-1</sup>. A 5 μL sample was injected into the column. Each compound was identified by comparison with the standards (glycerol, glyceric acid, glycolic acid, oxalic acid, tartronic acid, mesoxalic acid, glioxilic acid, lactic, formic acid, glyceraldehyde and dihydroxyacetone). Due to the difficult separation, and in order to confirm each peak, successive preparation of samples containing one additional standard (in growing time sequence) were injected. A PDA detector was used at different wavelength (190, 210, 225, 240 and 250 nm).

## 3. Results and disucssion

The actual compositions of the different monometallic catalysts are collected in Table 1. As it can be seen, in all the cases, there is a reasonable agreement between the nominal and the actual composition of the different catalysts, confirming the deposition of the metal nanoparticles on the carbon support. Pd percentage in the prepared Pt/C powders could not be quantified. However, the final weight of the prepared catalysts powders were very close to the theoretical ones, so that it will be assumed that the nominal and the actual metal percentage are approximately equals.

*Table 1: Nominal and actual composition of the different catalyst (Pd was not measured for the reasons abovementioned) and average particle size from TEM images*

| Catalyst | Nominal metal percentage | Actual metal percentage | Average particle size / nm |
|----------|--------------------------|-------------------------|----------------------------|
| Pt/C     | 20                       | 20.6                    | 3.2                        |
|          | 30                       | 29.4                    | 3.4                        |
|          | 40                       | 38.0                    | 2.8                        |
|          | 60                       | 58.1                    | 4.3                        |
| Au/C     | 10                       | 11.1                    | 4.6                        |
|          | 20                       | 21.8                    | 4.1                        |
|          | 30                       | 28.1                    | 3.7                        |
|          | 40                       | 42.3                    | 5.7                        |
| Pd/C     | 20                       |                         | 3.3                        |
|          | 30                       |                         | 4.8                        |
|          | 40                       | -                       | 6.5                        |
|          | 60                       |                         | 5.0                        |

The diffractograms of the different catalysts are presented in Figure 1. As it can be seen, in the case of the Pt/C and the Au/C catalysts, all of them present the typical peaks associated to the fcc unit cell structure. Figure 1 collects the position of the different peaks along with the crystal size estimated from the Scherrer equation (Araujo et al., 2013). In the case of the Pd/C catalysts, apart from the peaks associated to the metallic Pd fcc structure, other peaks appear, especially one very intense around 40.5°. Although the assignment of these is not clear, it has been reported in the literature the formation of some PdC during the preparation of Pd/C catalysts (Krishnankutty and Vannice, 1994). The authors reported a lattice expansion in the Pd crystalline structure due to the insertion of the carbon atoms, appearing new peaks in the diffractogram different to those of Pd fcc (see dotted lines Figure 1c). The crystal sizes for the Pt/C and Au/C are in the nanometric range (values collected in Table 1), with a slight increase with the metal loading, as expected from the smaller dispersion. In the case of the Pd/C, in spite of the lack of quantification, it can be qualitatively inferred that the catalysts is also formed by nanocrystals. The estimation of the average particle sizes from the TEM images is collected in Table 1. As it can be seen, all the materials present average particle size in the range of 3-7 nm, corroborating the deposition of metal nanoparticles on the carbon support.

The electrochemical activity of the different catalysts was assessed by cyclic voltammetry. As it can be seen, in terms of current density, the most active metal was the Au/C, where there is an optimum for the 20% Au/C (maximum current density of 6 A mg<sup>-1</sup>). However, the main limitation of this material is the high overpotential required for becoming active for glycerol electrooxidation, as stated by Angelucci et al. (2013), due the appearance of oxygenated species at higher potential compared to Pt.

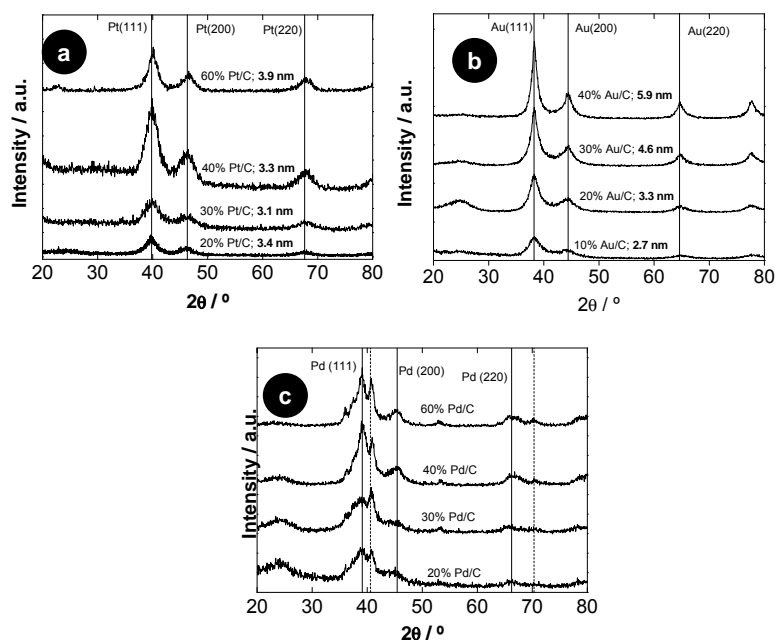


Figure 1. XRD patterns of the different prepared monometallic catalysts: a) Pt/C; b) Au/C; and c) Pd/C (dotted lines corresponds to palladium carbene reflections)

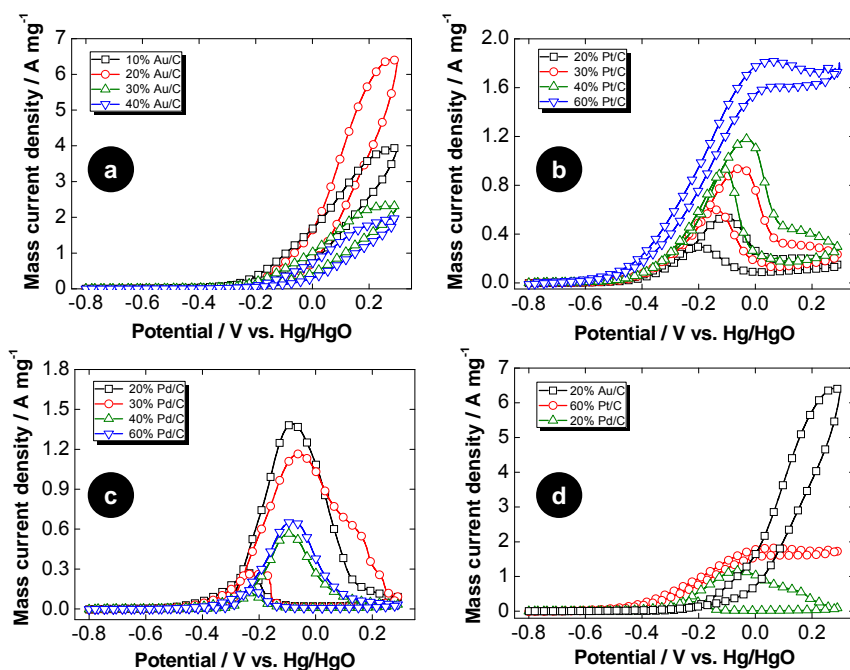


Figure 2. Cyclic voltammograms of the different catalysts: a) Au/C; b) Pt/C; c) Pd/C and d) the comparison for the best materials

In the case of the onset potential, Pt/C possesses the lowest values, around -0.5 V vs Hg/HgO. In terms of mass current density, 60% Pt/C demonstrated to be the most effective catalyst, with the highest current density compared to the other Pt loadings. In the case of the Pd/C, the onset potential for the glycerol electrooxidation presents intermediate values compared to Pt and Au, although in terms of mass current density, it appears to be the weakest material. Figure 2d compares the most efficient catalysts for each material, corroborating the trends here mentioned. The 60% Pt/C is the material earliest oxidizing glycerol (lowest onset potential), whereas the 20% Au/C is the most active one in terms of mass current density.

Figure 3 shows the results of the chronoamperometric studies and the product distribution carried out on the three most active materials at -0.2 V vs. Hg/HgO. As it can be seen, the material that displays the highest current density is the 60% Pt/C compared to Au/C and Pd/C. This again reflects that at low anodic potentials, more useful in practical fuel cell terms, the most effective material for glycerol electrooxidation is Pt/C, particularly the 60% Pt/C. Au/C displays a much lower current density, due to the low electrocatalytic activity at this anode potential (higher potentials are required for activating this material). In the case of Pd/C, despite the larger initial current compared to Au/C, it steeply drops down to values similar to that of Au/C. As mentioned by Zhang et al. (2013), the Pd surface can significantly get poisoned by the adsorbates produced during the glycerol electrooxidation.

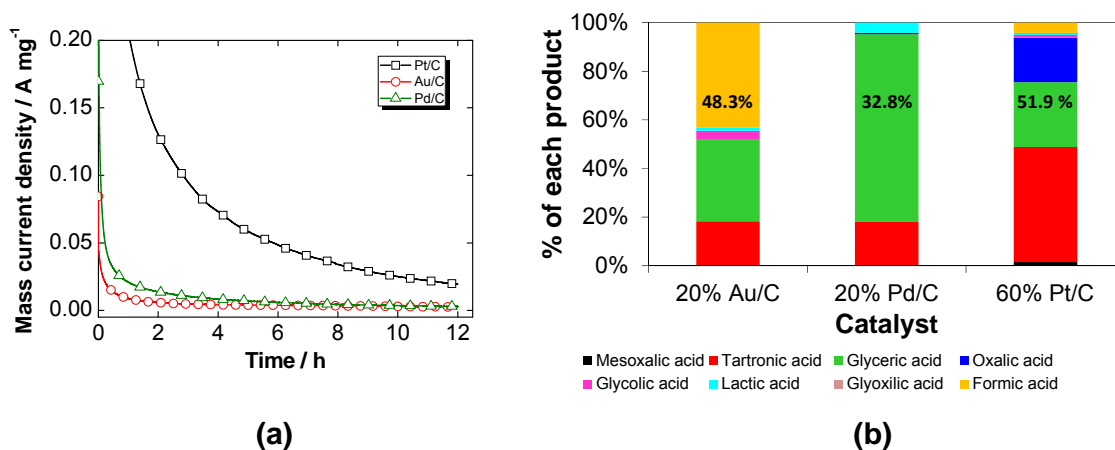


Figure 3. (a) Chronoamperometric curves of the different catalysts in  $1 \text{ mol L}^{-1}$  glycerol and  $1 \text{ mol L}^{-1}$  KOH at -0.2 V vs. Hg/HgO; and (b) Distribution of the products formed during the chronoamperometry (number corresponds to the Faradaic efficiency)

The distribution of products shows significant differences depending on the metal. In the case of the Au/C, there is a large production of formic acid as final product, which corresponds to a dissociative adsorption of the glycerol molecule on the Au active sites. Also, glyceric and tartronic acid appear as other relevant  $\text{C}_3$  organic acid products (Prati et al., 2011). In the case of the Pd/C, there is a very significant selectivity to the production of glyceric acid as the main oxidation product, achieving a value of 77%. Finally, in the case of Pt/C, the product distribution becomes more complex: the selectivity to tartronic acid achieves a value of 47%, followed by glyceric acid as second product. However,  $\text{C}_2$  acids are also formed, which is associated to a C-C scission and further oxidation of the  $\text{C}_2$  residue coming from glyceric or even tartronic acid. Also, a small percentage of formic acid is observed (Zhang et al., 2012). The different product distribution directly impacts on the Faradaic efficiency (percentage of electrons used over the 14 available for the complete glycerol electrooxidation), appearing Pt/C as the most efficient material for electrooxidizing glycerol.

#### 4. Conclusions

Monometallic Pt, Au and Pd supported on carbon nanoparticles can be easily prepared from simple and well-known chemical reduction method. Pt/C and Au/C displays the typical fcc crystalline structure, and only in the case of Pd/C is observed a possible presence of palladium carbide. In spite of this, the three materials possess catalytic activity for glycerol electrooxidation in alkaline medium. The Pt/C presents the lowest onset potential, whereas the highest activity (mass current density) is displayed for Au/C, with intermediate values for Pd/C. The most adequate metal loadings in the range of study are 60% Pt/C, 20% Au/C and 20% Pd/C. The chronoamperometric curves of these materials confirm that at relatively low potentials, Pt/C is the most active material. Finally, the products distribution reveal a significant selectivity

of Pd/C for producing glyceric acid, a large percentage of formic acid in the glycerol electrooxidation on gold, demonstrating the large capacity of this materials for cleaving C-C bonds, and a more complex distribution in the Pt/C, where almost 50% of the obtained products is tartronic acid. Hence, the product selectivity is greatly influenced, among other possible factors, by the electrocatalyst chosen.

### Acknowledgements

The authors want to thank the Conselho Nacional de Desenvolvimento Científico e Tecnológico (CNPq) for the financial support through the project (Universal Call 474381/2013-7).

### References

- Angelucci, C.A., Varela, H., Tremiliosi-Filho, G., Gomes, J.F., 2013, The significance of non-covalent interactions on the electro-oxidation of alcohols on Pt and Au in alkaline media, *Electrochemistry Communications*, 33,10-13.
- Beltrán-Prieto, J.C., Kolomazník, K.,Pecha, J., 2013, A review of catalytic systems for glycerol oxidation: Alternatives for waste valorization, *Australian Journal of Chemistry*, 66, 511-521.
- Cheng, N., Lv, H., Wang, W., Mu, S., Pan, M., Marken, F., 2010, An ambient aqueous synthesis for highly dispersed and active Pd/C catalyst for formic acid electro-oxidation, *Journal of Power Sources*, 195, 7246-7249.
- Garcia, R., Besson, M., Gallezot, P., 1995, Chemoselective catalytic oxidation of glycerol with air on platinum metals, *Applied Catalysis A-General*, 127,165-176.
- Issariyakul, T., Dalai, A.K., 2014, Biodiesel from vegetable oils, *Renewable Sustainable Energy Reviews*. 31, 446-471.
- Kiss, A.A., Ignat, R.M., 2012, Enhanced methanol recovery and glycerol separation in biodiesel production – DWC makes it happen, *Applied Energy* 99, 146-153.
- Krishnankutty, Nalini, Vannice, M.A., 1994, Palladium carbide formation in Pd/C catalysts and its effect on adsorption, absorption and catalytic behavior, *MRS Proceedings*, 368, 81.
- Lamy, C., Coutanceau, C., 2013, Electrocatalysis of alcohol oxidation reactions at platinum group metals, *RSC Energy and Environment Series*, 2013, 1-70.
- Mota, C.J.A., Silva, C.X.A.D., Gonçalves, V.L.C., 2009, Glycerochemistry: New Products and Processes from Glycerin of Biodiesel Production, *Quimica Nova*, 32, 639-648.
- Peuckert, M., 1985, XPS study on surface and bulk palladium oxide, its thermal stability, and a comparison with other noble metal oxides, *Journal of Physical Chemistry*, 89, 2481-2486.
- Pinheiro, A.L.N., Oliveira-Neto, A., De Souza, E.C., Perez, J., Paganin, V.A., Ticianelli, E.A., Gonzalez, E.R., 2003, Electrocatalysis on Noble Metal and Noble Metal Alloys Dispersed on High Surface Area Carbon, *Journal of New Materials for Electrochemical Systems*, 6, 1-8.
- Prati, L., Villa, A., Chan-Thaw, C.E., Arrigo, R., Wang, D., Su, D.S., 2011, Gold catalyzed liquid phase oxidation of alcohol: The issue of selectivity, *Faraday Discussions*, 152, 353-365.
- Qi, J., Xin, L., Zhang, Z., Sun, K., He, H., Wang, F., Chadderdon, D., Qiu, Y., Liang, C., Li, W., 2013, Surface dealloyed PtCo nanoparticles supported on carbon nanotube: Facile synthesis and promising application for anion exchange membrane direct crude glycerol fuel cell. *Green Chemistry*, 15, 1133-1137.
- Rocha, T.A., Ibanhi, F., Colmati, F., Linares, J.J., Paganin, V.A., Gonzalez, E.R., 2013, Nb as an influential element for increasing the CO tolerance of PEMFC catalysts. *Journal of Applied Electrochemistry*, 43, 817-827.
- Rodrigues de Oliveira, E.F., 2012, Síntese e Estudo da Atividade Eletrocatalítica de Nanopartículas com Estruturas do Tipo Core-Shell e Hollow para a Redução de O<sub>2</sub>, Master Thesis, Instituto de Química de São Carlos, Universidade de São Paulo.
- Yazdani, S.S., Gonzalez, R., 2007, Anaerobic fermentation of glycerol: a path to economic viability for the biofuels industry, *Current Opinion in Biotechnology*, 18, 213-219.
- Zhang, Z., Xin, L., Li, W., 2012, Electrocatalytic oxidation of glycerol on Pt/C in anion-exchange membrane fuel cell: Cogeneration of electricity and valuable chemicals, *Applied Catalysis B-Environmental*, 119-120, 40-48.
- Zhang, Z., Xin, L., Qi, J., Chadderdon, D.J., Li, W., 2013, Supported Pt, Pd and Au nanoparticle anode catalysts for anion-exchange membrane fuel cells with glycerol and crude glycerol fuels, *Applied Catalysis B-Environmental*, 136-137, 29-39.
- Zheng, Y., Chen, X., Shen, Y., 2008, 1. Commodity Chemicals Derived from Glycerol, an Important Biorefinery Feedstock, *Chemical Reviews*, 108, 5253–5277.